

# STEADY STATE TEMPERATURE DISTRIBUTION AND HEAT FLOW IN PRISMATIC BARS WITH ISOTHERMAL BOUNDARY CONDITIONS

M. J. BALCERZAK and S. RAYNOR

The Technological Institute, Northwestern University, Evanston, Illinois, U.S.A.

(Received 12 September 1960, and in revised form 4 February 1961)

**Abstract**—Steady state two-dimensional temperature distribution and heat flow in prismatic bars with isothermal boundary conditions and various external geometry were computed and tabulated. The method of conformal mapping was used.

**Résumé**—Le flux de chaleur et la distribution de température bidimensionnelle, en régime permanent, dans des barres prismatiques avec des conditions aux limites isothermes et des géométries extérieures variées ont été calculés et tabulés. La méthode de la représentation conforme a été utilisée.

**Zusammenfassung**—Mit Hilfe der konformen Abbildung wurde die stationäre zwei-dimensionale Temperaturverteilung und der Wärmefluss in prismatischen Körpern mit isothermer Begrenzung und verschiedenen äusseren Abmessungen berechnet und in Tabellen angegeben.

**Аннотация**—Дано аналитическое решение стационарного двухмерного температурного поля и определен тепловой поток в призматических брусках при изотермических граничных условиях и различной внешней геометрии брусков. Решение сопровождается расчётами, представленными в виде таблиц и рисунков.

## NOMENCLATURE

General		<i>n</i> sided regular polygon
<i>k</i> ,	thermal conductivity;	$A_n$ , coefficient of the <i>n</i> 'th term in a polynomial;
<i>L</i> ,	the axial dimension of a prismatic bar;	<i>a</i> , the shortest distance from the center to a side of a regular polygon;
<i>Q</i> ,	heat flow rate;	<i>j</i> , running index;
<i>S</i> ,	shape factor;	<i>n</i> , number of sides of polygon;
<i>T</i> ,	temperature at a point ( <i>x,y</i> );	$\rho$ , non-dimensional ratio of radii as defined by equation (4.1).
<i>T<sub>i</sub></i> ,	temperature at the inner boundary;	Rectangle
<i>T<sub>o</sub></i> ,	temperature at the outer boundary;	<i>a</i> , one half of the shorter side of a rectangle;
<i>w</i> ,	complex number in the $\phi, \Psi$ plane;	<i>b</i> , one half of the longer side of a rectangle;
<i>x,y</i> ,	Cartesian co-ordinates of a point;	<i>K</i> , a constant term as defined for a rectangle by equation (5.5a).
<i>z</i> ,	complex number in the <i>x,y</i> plane;	Eccentric circle
$\nabla^2$ ,	Laplacian operator;	$\epsilon$ , eccentricity ratio as defined in Fig. 9.
$\Delta$ ,	difference;	Ellipse
$\rho, \theta$ ,	polar co-ordinates of a point;	<i>a</i> , the major axis of the inner ellipse;
$\phi, \Psi$ ,	Cartesian co-ordinates of a point in the mapping plane;	
$\phi_0, \Psi_0$ ,	values of $\phi$ and $\Psi$ at the outer boundary;	
$\phi_i, \Psi_i$ ,	values of $\phi$ and $\Psi$ at the inner boundary.	

- b*, the minor axis of the inner ellipse;  
*c*, the major axis of the outer ellipse;  
*d*, the minor axis of the outer ellipse.

### STATEMENT OF THE PROBLEM

THE steady state temperature distribution and heat flow in prismatic bars of various cross-sections are to be investigated. The bar material is assumed to be homogeneous, isotropic and with temperature-independent properties. The heat flow is due to central heat sources uniformly distributed along the bar axis maintaining uniform surface temperature.

The geometrical shapes considered are:

Class 1—"n-sided" regular polygon with small circular hole in the center. Special cases: triangle, square, pentagon, hexagon, heptagon, octagon, nonagon, decagon, circle.

A circular bar with an eccentric hole.

Class 2—Rectangle with small circular hole in the center, and with variable "aspect ratio".

Class 3—Elliptical cross-sections with a confocal elliptical hole, and with a confocal slit (a slit connecting the foci of the ellipse) as inner boundaries.

### THEORETICAL CONSIDERATIONS

Solutions of the problems will be obtained by the method of conformal mapping. A short review of the method follows [1].

The temperature distribution in the systems satisfied Laplace's equation,

$$\nabla^2 T = \frac{\partial^2 T}{\partial x^2} + \frac{\partial^2 T}{\partial y^2} = 0$$

in the domain of the  $x, y$  plane with the temperature  $T = T_0$  and  $T = T_i$  along the boundaries  $\phi_0(x, y)$ , the outer boundary, and  $\phi_i(x, y)$ , the inner boundary, respectively.

It can be shown if  $\phi$  and  $\Psi$  form a new co-ordinate system given by

$$\phi = \phi(x, y)$$

$$\Psi = \Psi(x, y)$$

such that

$$w = \phi + i\Psi = f(x + iy) = f(\rho e^{i\theta}) = f(z)$$

with the conditions that  $f(z)$  is analytic and  $f'(z)$  is not equal to zero, then the temperature distribution in the new co-ordinate system also satisfies the Laplace's equation

$$\nabla^2 T = \frac{\partial^2 T}{\partial \phi^2} + \frac{\partial^2 T}{\partial \Psi^2} = 0$$

and the temperature at the boundary  $\phi = \phi_0$  is  $T_0$ , and correspondingly, at  $\phi = \phi_i$  is  $T_i$ , [2-4].

The application of this method is done by choosing a known solution in the  $\phi, \Psi$  plane, and by an appropriate choice of the mapping function,  $f(x + iy)$ .

The simplest solution in the  $\phi, \Psi$  plane is for one dimensional heat flow, with the boundary conditions that along  $\phi = \phi_0$ , the temperature is  $T_0$ , and along  $\phi = \phi_i$ , it is  $T_i$ . Then

$$T - T_0 = (T_i - T_0) \frac{\phi - \phi_0}{\phi_i - \phi_0} \quad (1)$$

The heat flow for the one dimensional case between the flow lines  $\Psi_1$ , and  $\Psi_2$  is, according to Fourier's Law, equal to

$$Q = k(T_i - T_0) \frac{\Delta\Psi}{\phi_0 - \phi_i} L \quad (2)$$

where  $L$  is the width of the bar and  $\Delta\Psi = \Psi_2 - \Psi_1$ .

It can be shown that the resultant heat flow computed in the  $\phi, \Psi$  plane is identical to the heat flow in the  $x, y$  plane. The heat flow per unit width is

$$\frac{Q}{L} = \frac{k\Delta\Psi}{\phi_0 - \phi_i} (T_i - T_0)$$

or

$$\frac{Q}{L} = kS(T_i - T_0)$$

where the shape factor,  $S$ , is defined as:

$$S = \frac{\Delta\Psi}{\phi_0 - \phi_i} \quad (3)$$

### STEADY TRANSVERSE HEAT FLOW IN PRISMATIC RODS WITH "n-SIDED" REGULAR POLYGON CROSS-SECTIONS

Consider a long regular prismatic rod with a concentric circular hole, Fig. 1. The temperatures at the inner circular boundary, and at the

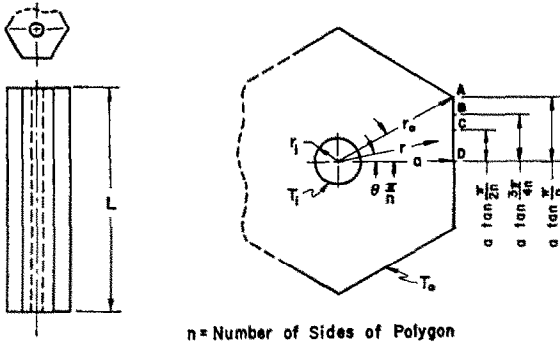


FIG. 1. Prismatic rod with "n-sided" regular polygonal cross-section.

outer prismatic boundary are  $T_i$  and  $T_o$  respectively.

The mapping function which transforms the one dimensional heat flow in the  $\phi, \Psi$  plane into the configuration of Fig. 1 is

$$w = \phi + i\Psi = 2 \ln z + \sum_{j=0}^{\infty} A_{jn} \rho^{jn} e^{ijn\theta} \quad (4.1)$$

$n =$  number of sides of polygon,

$$\rho = \frac{r}{r_o}$$

The choice of this particular mapping function was due to:

- (a) The influence of the power series diminishes toward the center. The lowest power of 3, for the case of a triangle, does not appreciably distort the temperature near the source.
- (b) The "n" fold symmetry accounts for the geometry of the "n-sided" polygon. On the outer boundary the contribution from the source is small compared with that from the power series.

The real part ( $\phi$ ) is:

$$\phi = \ln \rho^2 + A_0 + A_n \rho^n \cos n\theta + A_{2n} \rho^{2n} \cos 2n\theta + A_{3n} \rho^{3n} \cos 3n\theta + \dots \quad (4.2)$$

and the imaginary part ( $\Psi$ ) is:

$$\Psi = 2\theta + A_n \rho^n \sin n\theta + A_{2n} \rho^{2n} \sin 2n\theta + A_{3n} \rho^{3n} \sin 3n\theta + \dots \quad (4.3)$$

The coefficients  $A_0, A_n, A_{2n},$  and  $A_{3n}$  can be

computed to yield the value of  $T_o$  or ( $\phi_o = 0$ ) at the points A, B, C, and D, considering only the first five terms of the series solution, (4.2). The values of these coefficients are given in Table 1 for various values of "n".

Table 1. Coefficients  $A_0, A_n, A_{2n},$  and  $A_{3n}$  for various values of "n" to be used with equations (4.7) and (4.8)

n	$A_0$	$A_n$	$A_{2n}$	$A_{3n}$
3	1.13916	1.83402	1.09469	0.39984
4	0.54159	0.59131	0.05767	0.00796
5	0.32131	0.29838	-0.01111	0.01183
6	0.21339	0.18145	-0.01839	0.01355
7	0.15214	0.12233	-0.01704	0.01276
8	0.11397	0.08818	-0.01457	0.01123
9	0.08832	0.06642	-0.01218	0.00972
10	0.07076	0.05201	-0.01029	0.00841
.	.	.	.	.
.	.	.	.	.
.	.	.	.	.
$\infty$	0	0	0	0

The method described above results in an approximation, and the outer boundary temperature is equal to  $T_o$  at the few points selected. The maximum deviations from the constant value ( $T_o$ ) were computed for the triangle and square, expecting the largest error in these cases. The deviation is less than  $(T_i - T_o)/150$  in the case of the triangle, and  $(T_i - T_o)/2000$  for the square. Therefore, for all practical cases, along the outer prismatic boundary, the value of  $\phi$  is:

$$\phi_o = 0. \quad (4.4)$$

Along the inside circular boundary for small values of  $\rho_i$  ( $\rho_i \ll 1$ )

$$\phi_i = \ln \rho_i^2 + A_0 \quad (4.5)$$

resulting in a constant temperature along the inner circular boundary.

Since  $\theta$  varies from 0 to  $2\pi$  in the  $x, y$  plane, then from (4.3)

$$\Delta\Psi = 4\pi. \quad (4.6)$$

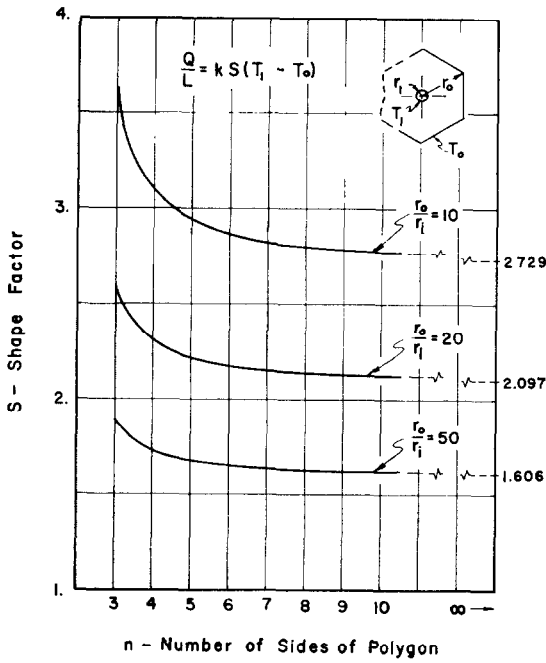


FIG. 2. Shape factor versus number of sides of regular polygon.

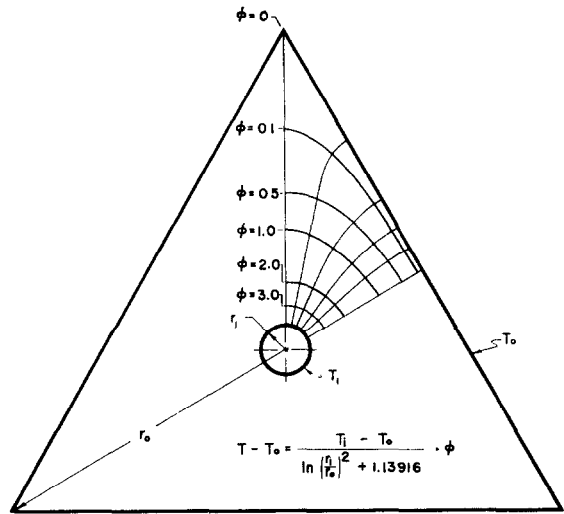


FIG. 3. Temperature distribution in a prismatic rod with triangular cross-section.

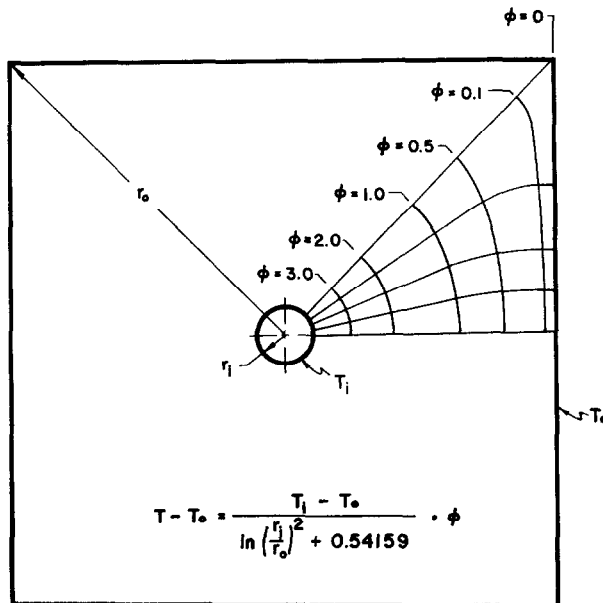


FIG. 4. Temperature distribution in a prismatic rod with square cross-section.

FIG. 5. Temperature distribution in a prismatic rod with pentagonal cross-section.

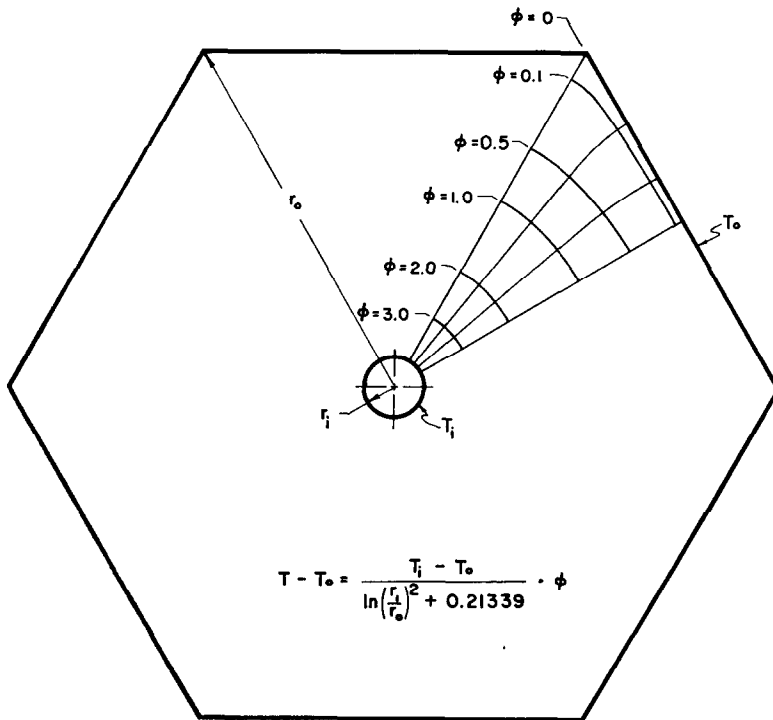
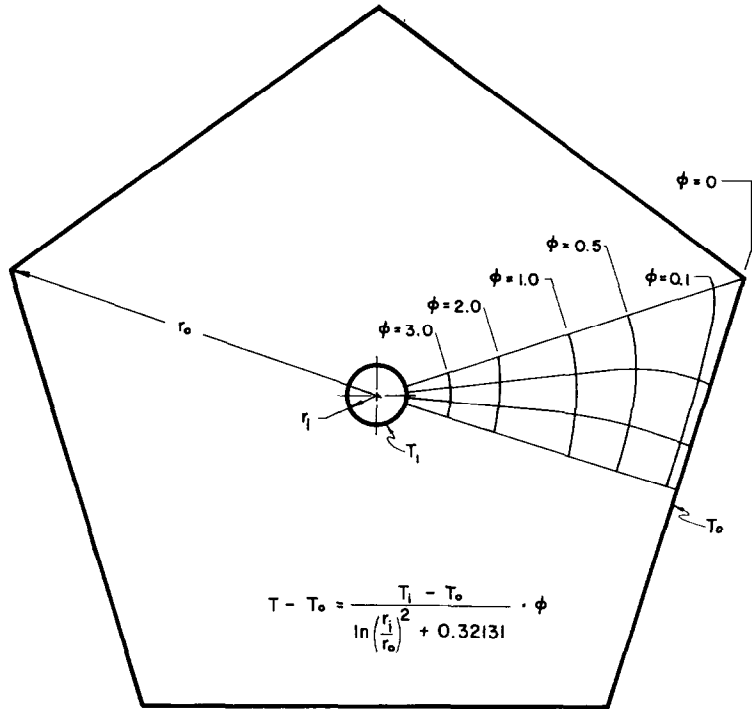


FIG. 6. Temperature distribution in a prismatic rod with hexagonal cross-section.

The temperature distribution is then obtained by substituting (4.2), (4.4), and (4.5) into (1).

$$T - T_0 = \frac{T_i - T_0}{\ln \frac{r_0}{r_i} + A_0} (\ln \rho^2 + A_0 + A_n \rho^n \cos n\theta + A_{2n} \rho^{2n} \cos 2n\theta + A_{3n} \rho^{3n} \cos 3n\theta) \quad (4.7)$$

and substituting (4.4), (4.5), and (4.6) into (3) yields the shape factor

$$S = \frac{2\pi}{\ln \frac{r_0}{r_i} - \frac{A_0}{2}} \quad (4.8)$$

It should be noted that  $A_0$  is the only coefficient affecting the value of the shape factor for  $r_i/r_0$  sufficiently small.

Values of the shape factor versus the number of sides of the polygon, "n", appear in Fig. 2. The temperature distribution for the triangle, square, pentagon, and hexagon are shown in Figs. 3, 4, 5 and 6.

Smith *et al.* [5] used an electrical analogue to determine the shape factor for a square with a central hole. From the graphical data, an empirical equation for the shape factor (written here with the notation used in this paper) was defined as

$$S = \frac{6.42}{\ln \frac{r_0}{r_i} - 0.264} \quad (4.9)$$

It is interesting to notice the close similarity of this equation to the equation (4.8) as re-written in the form

$$S = \frac{6.28318}{\ln \frac{r_0}{r_i} - 0.27079} \quad (4.10)$$

The agreement between the analysis and the experimental findings is excellent.

Moore [6] used field maps to study the problem of a square with a central hole. The result reported by Moore and Smith *et al.* show not only an excellent agreement for small values of  $r_i/a$ , but the agreement is close even for  $r_i/a = 0.7$ .

### STEADY TRANSVERSE HEAT FLOW IN PRISMATIC BARS WITH RECTANGULAR CROSS-SECTIONS

The configuration under study is represented in Fig. 7, and consists of a rectangle with sides  $2a$  and  $2b$ , having a circular inner boundary. The temperatures at the inner and outer boundaries are  $T_i$  and  $T_0$  respectively.

The mapping function which transforms the one-dimensional heat flow in the  $\phi, \Psi$  plane with constant temperatures at  $\phi_i$  and  $\phi_0$  to the configuration of Fig. 7 in the  $x, y$  plane is

$$w = \phi + i\Psi = 2 \sum_{n=0}^{\infty} (-1)^n \ln \left[ \coth \frac{\pi}{4a} (z \pm 2nb) \right] \quad (5.1)$$

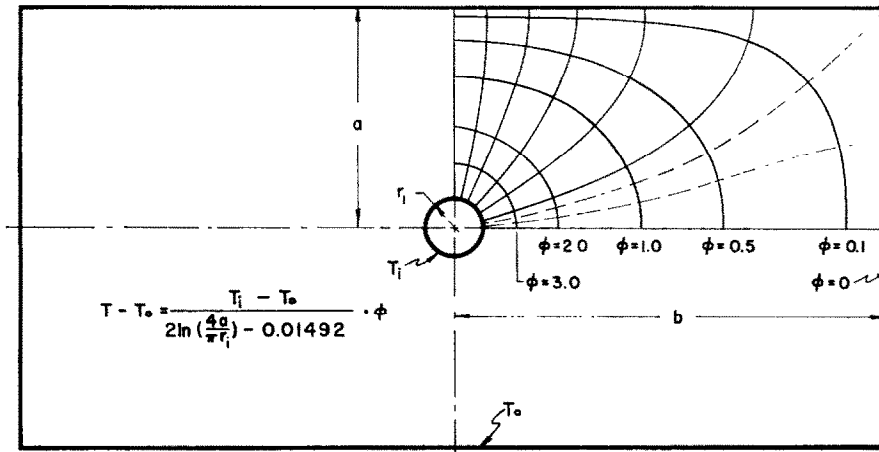


FIG. 7. Temperature distribution in a prismatic rod with rectangular cross-section ( $b/a = 2$ ).

This form of the mapping function was obtained by filling the  $x,y$  plane with an infinite matrix of sources and sinks spaced by  $2b$  in the  $x$  direction and by  $2a$  in the  $y$  direction.

The real part ( $\phi$ ) is:

$$\phi = \sum_{n=0}^{\infty} (-1)^n \ln \left[ \frac{1 + \frac{\cos \frac{\pi y}{2a}}{\cosh \frac{\pi}{2a} (x \pm 2nb)}}{1 - \frac{\cos \frac{\pi y}{2a}}{\cosh \frac{\pi}{2a} (x \pm 2nb)}} \right] \quad (5.2)$$

The imaginary part ( $\Psi$ ) is:

$$\Psi = 2 \sum_{n=0}^{\infty} (-1)^{n+1} \tan^{-1} \left[ \frac{\sin \frac{\pi y}{2a}}{\sinh \frac{\pi}{2a} (x \pm 2nb)} \right] \quad (5.3)$$

The value of  $\phi$  at the outer boundary of the rectangle is:

$$\phi_0 = 0 \quad (5.4)$$

at the inner circular boundary, when  $r_i/2 \ll 1$ , (or  $x/a \ll 1, y/a \ll 1$ ),  $\phi$  converges from (5.2) to

$$\phi_i = 2 \ln \frac{4a}{\pi r_i} - 4 \sum_{m=0}^{\infty} \sum_{n=1}^{\infty} \frac{(-1)^{n+1}}{(2m+1)} \operatorname{sech}^{(2m+1)} \frac{n\pi b}{a} \quad (5.5)$$

The double-summed term can be shown to be convergent and it will henceforth be denoted by  $K$ , so that

$$\phi_i = 2 \ln \frac{4a}{\pi r_i} - 4K \quad (5.5a)$$

where:

$$K = \sum_{m=0}^{\infty} \sum_{n=1}^{\infty} \frac{(-1)^{n+1}}{(2m+1)} \operatorname{sech}^{(2m+1)} \frac{n\pi b}{a}$$

The values of  $K$  are listed in Table 2 for various  $b/a$  ratios.

Table 2. Values of  $K$  for various  $b/a$  ratios to be used with equations (5.7) and (5.8)

$\frac{b}{a}$	$K$
1.00	0.08290
1.25	0.03963
1.50	0.01781
1.75	0.00816
2.00	0.00373
2.25	0.00170
2.50	0.00078
3.00	0.00016
4.00	$6.9748 \times 10^{-6}$
5.00	$3.0140 \times 10^{-7}$
10.00	$4.5422 \times 10^{-14}$
$\vdots$	$\vdots$
$\infty$	0

The variation of  $\theta$  in the  $x,y$  plane from 0 to  $2$  corresponds to a variation in the  $\phi, \Psi$  plane from  $\Psi_1 = 0$  to  $\Psi_2 = -4\pi$ . Thus

$$\Delta\Psi = -4\pi \quad (5.6)$$

The temperature distribution is then given by substituting (5.2), (5.4), and (5.5) into (1):

$$T - T_0 = \frac{T_i - T_0}{2 \ln \frac{4a}{\pi r_i} - 4K}$$

$$\times \sum_{n=0}^{\infty} (-1)^n \ln \left[ \frac{1 + \frac{\cos \frac{\pi y}{2a}}{\cosh \frac{\pi}{2a} (x \pm 2nb)}}{1 - \frac{\cos \frac{\pi y}{2a}}{\cosh \frac{\pi}{2a} (x \pm 2nb)}} \right] \quad (5.7)$$

The shape factor is obtained by substituting (5.4), (5.5) and (5.6) into (3):

$$S = \frac{2\pi}{\ln \frac{4a}{\pi r_i} - 2K} \quad (5.8)$$

The temperature distribution is illustrated for  $b/a = 2$  in Fig. 7, and the values of the shape factor versus aspect ratio  $b/a$  are plotted in Fig. 8.

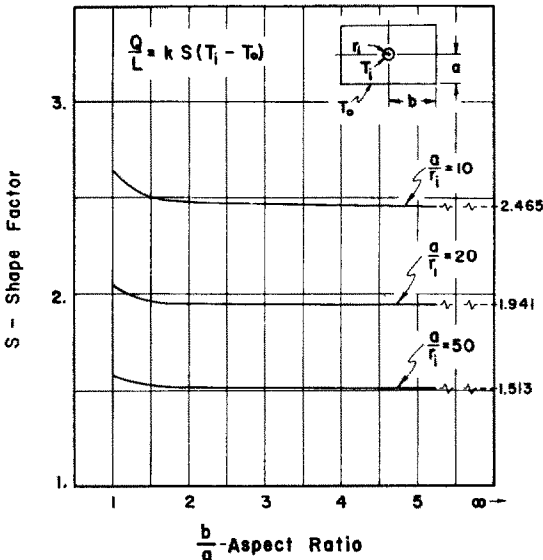


FIG. 8. Shape factor versus aspect ratio of rectangular.

When  $b/a$  tends to infinity, the temperature distribution of (5.7) and the shape factor,  $S$ , as given by (5.8), describe the case of an infinitely long strip with an inner circular boundary on the center line of the strip.

#### STEADY TRANSVERSE HEAT FLOW BETWEEN ECCENTRIC CIRCULAR CYLINDERS

Consider a bar with a circular outer boundary, and an eccentric circular inner boundary. The outer and inner boundary temperatures are  $T_0$  and  $T_i$  respectively.

This problem is briefly discussed in Carslaw and Jaeger [2], and is quoted here briefly for the sake of completeness only.

The values of the shape factor versus eccentricity ratio,  $\epsilon$ , are plotted in Fig. 9.

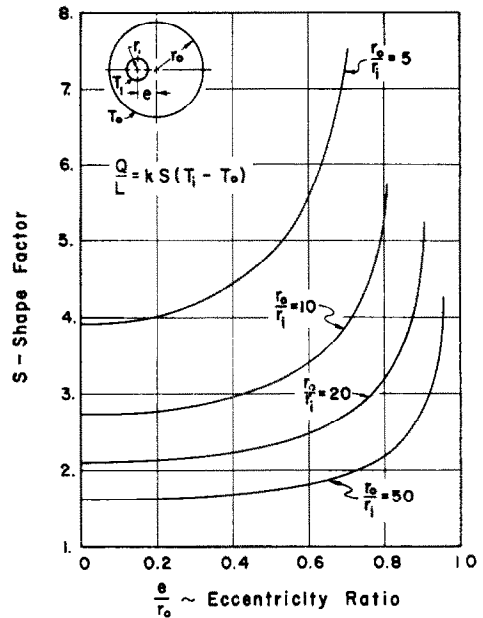


FIG. 9. Shape factor versus eccentricity ratio.

#### STEADY TRANSVERSE HEAT FLOW IN PRISMATIC BARS WITH ELLIPTICAL CROSS-SECTIONS

Consider a prismatic bar with confocal elliptical inner and outer boundaries. The temperatures of the outer and inner boundaries are  $T_0$  and  $T_i$ , respectively.

The mapping function which transforms the one-dimensional heat flow in the  $\phi, \Psi$  plane with constant temperatures at  $\phi_i$  and  $\phi_0$  to the configuration of Fig. 10 in the  $x, y$  plane is [7]:

$$w = \phi + i\Psi = -i \sin^{-1} \frac{z}{f}. \quad (7.1)$$

The expressions for  $\phi$  and  $\Psi$  are given in the implicit form

$$\frac{x^2}{f^2 \cosh^2 \phi} + \frac{y^2}{f^2 \sinh^2 \phi} = 1 \quad (7.2)$$

and

$$\frac{x^2}{f^2 \sin^2 \Psi} - \frac{y^2}{f^2 \cos^2 \Psi} = 1. \quad (7.3)$$

Along the outer boundary

$$\phi_0 = \tanh^{-1} \frac{d}{c} \quad (7.4)$$



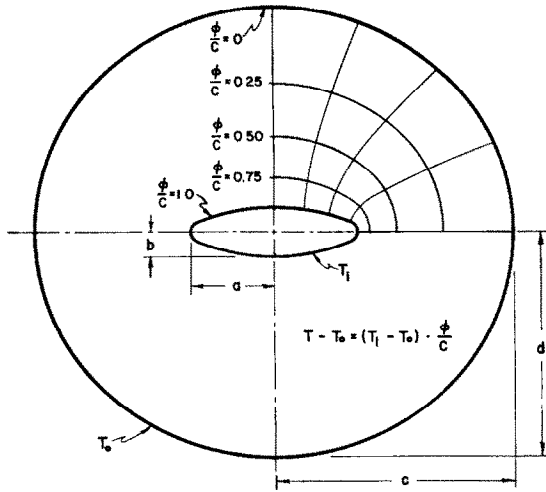


FIG. 10. Temperature distribution in a prismatic rod with confocal elliptical cross-section ( $c/d = 1.058$ ;  $b/d = 0.10$ ).

and along the inner boundary

$$\phi_i = \tanh^{-1} \frac{b}{a} \tag{7.5}$$

where

$$c^2 - d^2 = f^2$$

$$a^2 - b^2 = f^2.$$

The values of  $\Psi$  undergo a change of

$$\Delta\Psi = 2\pi. \tag{7.6}$$

The temperature distribution is given by substituting (7.4) and (7.5) into (1):

$$T - T_0 = (T_i - T_0) \frac{\phi - \ln \frac{c+d}{f}}{\ln \frac{a+b}{c+d}}. \tag{7.7}$$

The appropriate value of  $\phi$  can be determined from (7.2) for particular values of  $x$  and  $y$ .

The shape is obtained by substituting (7.4), (7.5), and (7.6) into (3):

$$S = \frac{2\pi}{\ln \frac{c+d}{a+b}} \tag{7.8}$$

The temperature distribution is shown in Fig. 10, and the shape factor is plotted versus the ratio of major to minor axis,  $c/d$ , in Fig. 11.

The case of the inner boundary degenerating into the focal slit, a slit connecting the foci of the

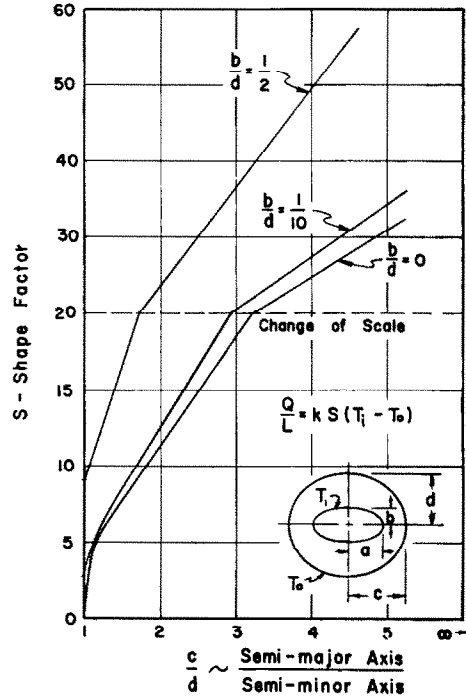


FIG. 11. Shape factor versus  $c/d$  ratio of confocal ellipses.

outer elliptic boundary, is given by the curve  $b/d = 0$ .

### SUMMARY

The temperature distribution and the heat flow for long prismatic bars with constant temperatures at the outer and inner boundaries were computed and the results are summarized in Table 3.

### ACKNOWLEDGEMENT

The authors would like to express their thanks to the Transportation Center at Northwestern University for supporting this study.

Table 3. Summary of results

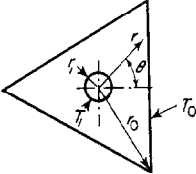
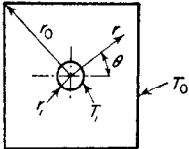
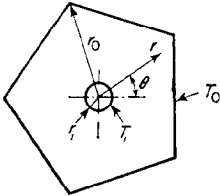
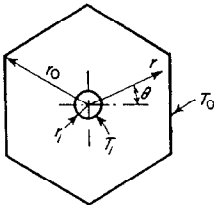
Shape and notation	Temperature distribution	Shape factor, $S$ $\frac{Q}{L} = kS(T_i - T_0)$
 <p data-bbox="225 579 303 604">Triangle</p>	$T - T_0 = \frac{T_i - T_0}{\ln \left( \frac{r_i}{r_0} \right)^2 + 1.13916} \left[ \ln \left( \frac{r}{r_0} \right)^2 + 1.13916 \right.$ $+ 1.83402 \left( \frac{r}{r_0} \right)^3 \cos 3\theta + 1.09469 \left( \frac{r}{r_0} \right)^6 \cos 6\theta$ $\left. + 0.39984 \left( \frac{r}{r_0} \right)^9 \cos 9\theta \right]$	$\frac{2\pi}{\ln \frac{r_0}{r_i} - 0.56958}$
 <p data-bbox="232 895 297 920">Square</p>	$T - T_0 = \frac{T_i - T_0}{\ln \left( \frac{r_i}{r_0} \right)^2 + 0.54159} \left[ \ln \left( \frac{r}{r_0} \right)^2 + 0.54159 \right.$ $+ 0.59131 \left( \frac{r}{r_0} \right)^4 \cos 4\theta + 0.05767 \left( \frac{r}{r_0} \right)^8 \cos 8\theta$ $\left. + 0.00796 \left( \frac{r}{r_0} \right)^{12} \cos 12\theta \right]$	$\frac{2\pi}{\ln \frac{r_0}{r_i} - 0.27079}$
 <p data-bbox="220 1229 306 1253">Pentagon</p>	$T - T_0 = \frac{T_i - T_0}{\ln \left( \frac{r_i}{r_0} \right)^2 + 0.32131} \left[ \ln \left( \frac{r}{r_0} \right)^2 + 0.32131 \right.$ $+ 0.29838 \left( \frac{r}{r_0} \right)^5 \cos 5\theta - 0.0111 \left( \frac{r}{r_0} \right)^{10} \cos 10\theta$ $\left. + 0.01183 \left( \frac{r}{r_0} \right)^{15} \cos 15\theta \right]$	$\frac{2\pi}{\ln \frac{r_0}{r_i} - 0.16066}$
 <p data-bbox="223 1562 303 1586">Hexagon</p>	$T - T_0 = \frac{T_i - T_0}{\ln \left( \frac{r_i}{r_0} \right)^2 + 0.21339} \left[ \ln \left( \frac{r}{r_0} \right)^2 + 0.21339 \right.$ $+ 0.18145 \left( \frac{r}{r_0} \right)^8 \cos 6\theta - 0.01839 \left( \frac{r}{r_0} \right)^{12} \cos 12\theta$ $\left. + 0.01355 \left( \frac{r}{r_0} \right)^{18} \cos 18\theta \right]$	$\frac{2\pi}{\ln \frac{r_0}{r_i} - 0.10669}$

Table 3—continued

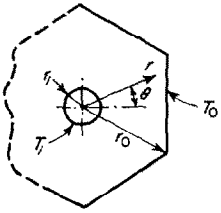
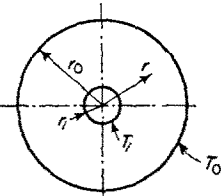
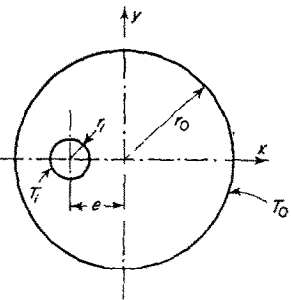
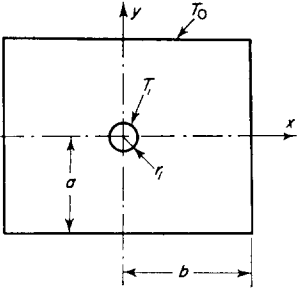
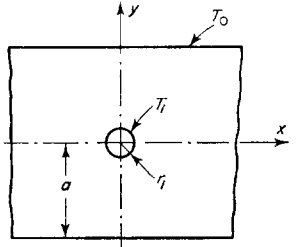
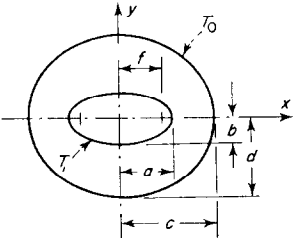
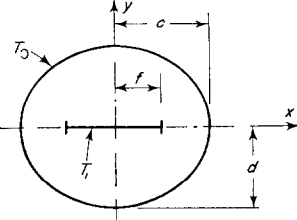
Shape and notation	Temperature distribution	Shape factor, $S$ $\frac{Q}{L} = kS(T_i - T_0)$
 <p>“<math>n</math>-Sided” regular polygon <math>n = \text{no. of sides}</math></p>	$T - T_0 = \frac{T_i - T_0}{\ln \left(\frac{r_o}{r_i}\right)^2 + A_0} \left[ \ln \left(\frac{r}{r_o}\right)^2 + A_0 \right.$ $+ A_n \left(\frac{r}{r_o}\right)^n \cos n\theta + A_{2n} \left(\frac{r}{r_o}\right)^{2n} \cos 2n\theta$ $\left. + A_{3n} \left(\frac{r}{r_o}\right)^{3n} \cos 3n\theta \right]$ <p>(See Table 1 for <math>A_0</math>, <math>A_n</math>, <math>A_{2n}</math>, and <math>A_{3n}</math>)</p>	$\frac{2\pi}{\ln \frac{r_o}{r_i} - \frac{A_0}{2}}$
 <p>Concentric circles</p>	$T - T_0 = (T_i - T_0) \frac{\ln \frac{r}{r_o}}{\ln \frac{r_o}{r_i}}$	$\frac{2\pi}{\ln \frac{r_o}{r_i}}$
 <p>Eccentric circles</p>	$T - T_0 = \frac{T_i - T_0}{2 \cosh^{-1} \left( \frac{1 + \rho_i^2 - \epsilon^2}{2\rho_i} \right)} \left[ \ln \frac{\left( \frac{x}{r_o} + \frac{h}{r_o} + \frac{a}{r_o} \right)^2 + \left( \frac{y}{r_o} \right)^2}{\left( \frac{x}{r_o} + \frac{h}{r_o} - \frac{a}{r_o} \right)^2 + \left( \frac{y}{r_o} \right)^2} \right.$ $\left. - \cosh^{-1} \left( \frac{1 - \rho_i^2 + \epsilon^2}{2\epsilon} \right) \right]$ <p>Where:</p> $\rho_i = \frac{r_i}{r_o}; \quad \epsilon = \frac{e}{r_o}$ $\left(\frac{a}{r_o}\right)^2 = \frac{(1 - \rho_i^2 + \epsilon^2)^2}{4\epsilon^2} - 1$ $\frac{h}{r_o} = \frac{1 - \rho_i^2 + \epsilon^2}{2\epsilon}$	$\frac{2\pi}{\cosh^{-1} \left( \frac{1 + \rho_i^2 - \epsilon^2}{2\rho_i} \right)}$

Table 3—continued

Shape and notation	Temperature distribution	Shape factor, $S$ $\frac{Q}{L} = kS(T_i - T_0)$
 <p>Rectangle</p>	$T - T_0 = \frac{T_i - T_0}{2 \ln \frac{4a}{\pi r_i} - 4K} \sum_{n=0}^{\infty} (-1)^n \ln \left[ \frac{1 + \frac{\cos \frac{\pi y}{2a}}{\cosh \frac{\pi}{2a} (x \pm 2nb)}}{1 - \frac{\cos \frac{\pi y}{2a}}{\cosh \frac{\pi}{2a} (x \pm 2nb)}} \right]$ <p>(See Table 2 for <math>K</math>)</p>	$\ln \frac{2\pi}{\pi r_i} - 2K$
 <p>Infinite strip</p>	$T - T_0 = \frac{T_i - T_0}{2 \ln \frac{4a}{\pi r_i}} \ln \left[ \frac{1 + \frac{\cos \frac{\pi y}{2a}}{\cosh \frac{\pi x}{2a}}}{1 - \frac{\cos \frac{\pi y}{2a}}{\cosh \frac{\pi x}{2a}}} \right]$	$\ln \frac{2\pi}{\pi r_i} - 4a$
 <p>Confocal ellipses</p>	$T - T_0 = \frac{T_i - T_0}{\ln \frac{c+d}{c-d}} \left( \phi - \ln \frac{c+d}{f} \right)$ <p>Compute <math>\phi</math> from: <math>\frac{x^2}{f^2 \cosh^2 \phi} + \frac{y^2}{f^2 \sinh^2 \phi} = 1</math></p>	$\ln \frac{2\pi}{a} \frac{d}{b}$
 <p>Ellipse with focal slit</p>	$T - T_0 = \frac{T_i - T_0}{\ln \frac{c+d}{c-d}} \left( \phi - \ln \frac{c-d}{f} \right)$ <p>Compute <math>\phi</math> from: <math>\frac{x^2}{f^2 \cosh^2 \phi} + \frac{y^2}{f^2 \sinh^2 \phi} = 1</math></p>	$\ln \frac{2\pi}{c} \frac{d}{f}$

## REFERENCES

1. L. BIERBERBACH, *Conformal Mapping*. Chelsea Publishing, New York (1953).
2. H. S. CARSLAW and J. C. JAEGER, *Conduction of Heat in Solids*, 2nd Ed., pp. 421-454. Oxford University Press, London (1959).
3. E. R. G. ECKERT and R. M. DRAKE, JR., *Heat and Mass Transfer*, pp. 64-69. McGraw-Hill, New York (1959).
4. M. JAKOB, *Heat Transfer, Vol. I*, pp. 326-331. John Wiley, New York (1949).
5. J. C. SMITH, T. E. LIND, JR. and D. S. LERMOND, Shape factors for conductive heat flow, *J. Amer. Inst. Chem. Engrs*, **4**, 330-331 (1958).
6. A. D. MOORE, *Heat Transfer Notes for Electrical Engineering*, pp. 7-9. George Wahr, Ann Arbor, Michigan (1938).
7. R. V. CHURCHILL, *Introduction to Complex Variables and Applications*. McGraw-Hill, New York (1948).